

# Mid-IR Soliton Microcomb Generation in Silicon Nitride Microring Resonators

Anamika Karunakaran<sup>(1,2)</sup>, Marco Clementi<sup>(3)</sup>, Ozan Yakar<sup>(3)</sup>, Christian Lafforgue<sup>(3)</sup>, Anton Stroganov<sup>(4)</sup>, Poul Varming<sup>(1)</sup>, Minhao Pu<sup>(2)</sup>, Patrick Montague<sup>(1)</sup>, Kresten Yvind<sup>(2)</sup>, Camille-Sophie Brès<sup>(3)</sup>

<sup>(1)</sup> NKT Photonics, Blokken 84,3460 Birkerød, Denmark, [anamika.nair.karunakaran@nktphotonics.com](mailto:anamika.nair.karunakaran@nktphotonics.com)

<sup>(2)</sup> DTU Electro, Technical University of Denmark, 2800 Kgs. Lyngby, Denmark,

<sup>(3)</sup> École Polytechnique Fédérale de Lausanne, Photonic Systems Laboratory (PHOSL), CH-1015 Lausanne, Switzerland

<sup>(4)</sup> LIGENEC SA, EPFL Innovation Park, CH-1024 Ecublens, Switzerland

**Abstract** We demonstrate soliton Kerr-comb generation in a high-Q silicon nitride microring with 143 GHz free spectral range pumped at 1970 nm. The resulting low noise ultrafast pulse train displays a 422 nm bandwidth, extending up to 2250 nm.

©2023 The Authors

## Introduction

Optical frequency combs are coherent light sources with equally spaced frequency components. Since their breakthrough more than two decades ago, they have been found useful in a variety of applications ranging from metrology<sup>[1]</sup>, to spectroscopy and medical diagnostics<sup>[2]</sup>.

Frequency combs from microresonators, or Kerr microcombs, have generated a widespread research interest ever since their inception. In comparison with initial frequency combs, which were based on mode locked lasers, Kerr microcombs offer higher comb line spacing (from THz to 10's of GHz) with low optical power requirement and compactness. Notably, the usage of high-Q microresonators, enabled by recent progress in nanofabrication, allows to achieve a high comb coherence, that is necessary for applications such as astrocombs<sup>[3]</sup>, telecommunications<sup>[4]</sup>, data centers<sup>[5]</sup> and spectroscopy<sup>[6]</sup>, to name a few.

The vast majority of work has shown the operation of Kerr microcombs pumped at telecom wavelengths, either in the C/L band or in the O-band<sup>[7]</sup>, leveraging the availability of equipment and pump sources necessary to drive and characterize the integrated devices. While broadband Kerr combs, such as octave spanning microcombs, can be obtained in high quality (Q) factor microresonators, there is interest in developing Kerr microcombs directly operating outside the telecom band, for example towards the middle infrared (mid-IR). This is for example critical for spectroscopy as the mid-IR region hosts various and strong molecular absorption lines<sup>[8]</sup>. Overall, frequency combs in this wavelength range

are relatively less explored. A comb at 2.5  $\mu\text{m}$ , spanning 200 nm with 100 GHz repetition rate was demonstrated but in a crystalline microresonator<sup>[9]</sup>, hence difficult to integrate. A soliton microcomb spanning 330 nm was also generated by pumping near 2  $\mu\text{m}$  in a lithium niobate on insulator (LNOI) microresonator<sup>[10]</sup>. The dispersion engineering as well as fabrication of LNOI integrated devices is still at the moment very challenging.

In this work, we show for the first time, to the best of our knowledge, soliton Kerr comb generation in a 143 GHz free spectral range (FSR) silicon nitride ( $\text{Si}_3\text{N}_4$ ) microring resonators, with a pump wavelength close to 2  $\mu\text{m}$ . The comb spans 422 nm (31 THz), limited by the generation of a dispersive wave near 2.2  $\mu\text{m}$ . Further optimization of dispersion should allow pushing the operation deeper in the mid-IR. Our work extends  $\text{Si}_3\text{N}_4$  Kerr combs towards the mid-IR, adding new opportunities for the  $\text{Si}_3\text{N}_4$  platform.

## Microresonator and characterization

The  $\text{Si}_3\text{N}_4$  microresonators used in this experiment (Fig. 1a) were manufactured through a commercial-grade, multi-project wafer fabrication run at LIGENEC SA, using the AN800 process. The ring waveguide has a width of 1.7  $\mu\text{m}$  and height of 0.8  $\mu\text{m}$ . The resonators display a radius of 158  $\mu\text{m}$ , and gap of 700 nm between the bus and the ring. The calculated group velocity dispersion profile ( $\beta_2$ ) of the ring is shown in Fig. 1b along with the integrated dispersion ( $\beta_{int}$ ). For the chosen geometry, the resonator exhibits anomalous dispersion at wavelengths close to 2  $\mu\text{m}$ , with a zero-crossing close to 2.1  $\mu\text{m}$ . From the  $\beta_{int}$ , a dispersive wave is expected near 2.2  $\mu\text{m}$ . The

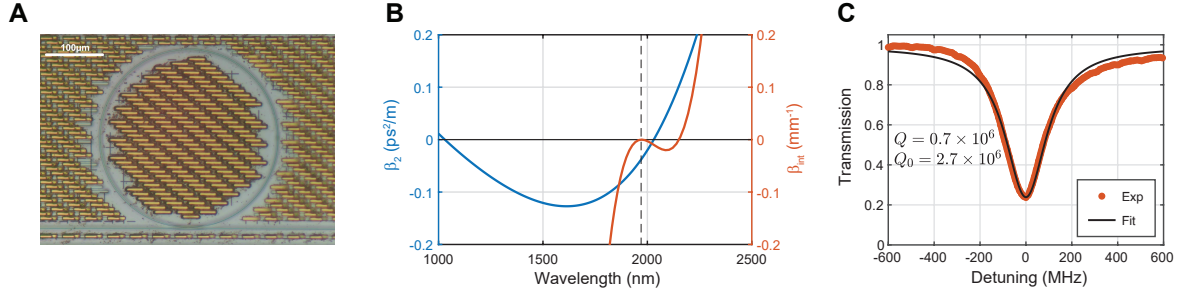


**Fig. 1:** (a) Microscope image of the  $\text{Si}_3\text{N}_4$  microring resonator. (b) Calculated group velocity dispersion (blue) and integrated dispersion (red) for pumping at 1970 nm (dashed line). (c) Normalized transmission spectrum at low power (center wavelength: 1969.5 nm).

FSR is calculated to be around 143 GHz in the target wavelength range. Light is edge-coupled to the photonic chip using a lensed fiber. An inverse taper is used to match the fundamental TE mode at the chip facet with the one of the fiber, resulting in an overall in-coupling loss of about 3 dB. The out-coupled light is collected using an aspheric convex lens and coupled into an optical fiber through a collimator. The pump laser is a NKT single frequency laser operating at 1970 nm.

The Q factor of the resonance was first assessed by coupling a few milliwatts of the 1970 nm laser light modulated at a fixed RF frequency while finely scanning its wavelength using a piezo-actuator, in order to record the transmission of the resonator<sup>[11]</sup>. The output of the microresonator was then recorded using a photodiode and an oscilloscope. Fitting the acquired data to a Lorentzian function, we calculated the linewidth of the resonance to be 209 MHz and the Q to be  $7.2 \times 10^5$  as shown in Fig. 1c. By taking into account the non-zero transmission of the device at the resonance wavelength, and assuming to operate in the overcoupled regime, we estimate an intrinsic quality factor ( $Q_0$ ) as high as  $2.7 \times 10^6$ .

### Soliton generation

Frequency combs are generated in a microresonator as a result of four-wave mixing process owing to the nonlinear properties of the material medium. The high third-order nonlinearity and high Q of  $\text{Si}_3\text{N}_4$  resonators significantly favor the process in our system. The dynamics of microresonator-based comb generation can be modelled using Lugiato-Lefever equations and for anomalous dispersion resonators, the stable solutions are predicted on the red side of the resonance<sup>[12]</sup>. The access to the soliton state is hence complicated by the sudden drop in intracavity power once they are generated and the subsequent resonance shift from thermal effects.

In our system, to counteract the shifting of the

resonance we used a pump/auxiliary laser technique for soliton generation<sup>[13]</sup>. While scanning the wavelength of the pump laser from blue to red, the resonance shifts will drag an auxiliary laser out of the auxiliary resonance. As the pump laser is tuned across the resonance to the effective red side, the auxiliary resonance will recoil bringing the auxiliary laser back into the resonance. Thus, by placing the auxiliary laser on the blue side of the 1550 nm resonance, the soliton states on the red side of the resonance become more accessible.

The setup is shown in Fig. 2a. The NKT single frequency laser at 1970 nm, amplified with a thulium doped fiber amplifier to have an on-chip power of 22 dBm, was used as the pump to generate the comb lines. An external cavity laser, amplified to 29 dBm, tuned near 1550 nm was used as an auxiliary laser. The wavelength of the pump laser was tuned using a function generator that controlled by the internal piezo. The two beams were combined using a wavelength division multiplexer (WDM) and coupled into the microresonator after a polarization controller. The output light of the microresonator was collected using a convex lens which had little transmission at 1550nm. The light was then coupled into a fiber after a collimator and then sent through a second WDM to split the 1970nm light from 1550 nm light. A portion of this light was sent to the optical spectrum analyser (OSA) to observe the spectrum. The rest of the output light was sent through a fiber Bragg grating to filter out the pump wavelength and monitor the converted power on an oscilloscope.

To generate the soliton Kerr comb, the pump laser was initially swept across pump resonance using a triangular signal driving the piezo controller of the laser while the auxiliary laser was tuned into the resonance manually. The converted power trace recorded at the oscilloscope is shown in Fig. 2b. The discontinuous steps

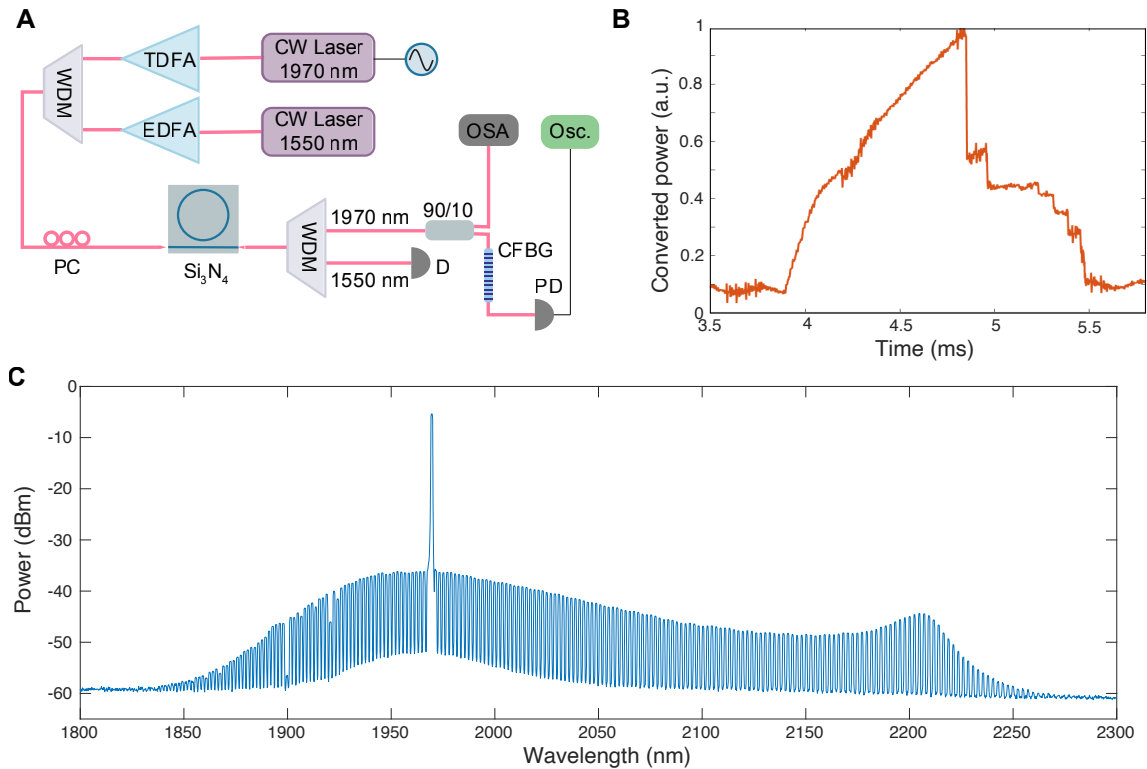


**Fig. 2:** (a) Experimental setup for mid-IR frequency comb generation in  $\text{Si}_3\text{N}_4$  ring resonators. EDFA: Erbium-doped fiber amplifier, TDFA: Thulium-doped fiber amplifier, WDM: Wavelength Division Multiplexer, 90/10: 90/10 coupler, OSA: Optical Spectrum Analyser, Osc.: Oscilloscope, CFBG: Chirped Fiber Bragg Grating, PD: Photodetector, D: Power meter. (b) Converted power trace over time representing different soliton states measured at PD. (c) Optical spectrum of a single soliton state.

seen on the red side of the resonance correspond to different soliton states with varying number of solitons circulating inside the cavity. The position of the auxiliary laser was fixed at the wavelength where soliton steps with the longest duration were observed. Afterwards, the wavelength sweep of the pump laser was switched off and this laser was manually tuned into resonance from the blue side. The solitons were accessible on the red side of the resonance with forward tuning of the pump.

The spectrum of the single soliton generated from this device is shown in Fig. 2c. This spectrum corresponds to the lowest step of the converted power trace in Fig. 2b and extends from 1840 nm to 2262 nm, spanning 422 nm. The comb line spacing is 143 GHz. The spectrum has a  $\text{sech}^2$  profile with a dispersive wave generated around 2200 nm, in agreement with the calculated integrated dispersion (Fig. 1b).

## Conclusions

We show the generation of a bright soliton Kerr microcomb pumped at 1970 nm in a 150 GHz  $\text{Si}_3\text{N}_4$  microring. The ring, with dimensions of  $1.7 \times 0.8 \mu\text{m}^2$ , was chosen to display anomalous dispersion at the pump wavelength. The large gap, 700 nm, enabled good coupling of the 1970 nm

light to the ring, which exhibited a Q factor of  $0.72 \times 10^6$ . The obtained soliton has a spectrum reaching up to 2262 nm, in perfect agreement with the predicted dispersive wave. This first demonstration in  $\text{Si}_3\text{N}_4$  shows that the platform provides the required low loss and nonlinearity at long wavelengths, even in relatively small FSR rings. Further dispersion optimization should allow pushing the comb generation further into the mid-IR, opening the way for the integrated of mid-IR frequency combs.

## Acknowledgement

This work was supported by H2020 Marie Skłodowska-Curie Actions grant MEFISTA (861152) and ERC grant PISSARRO (ERC-2017-CoG 771647).

## References

- [1] A. D. Ludlow, M. M. Boyd, J. Ye, E. Peik, and P. O. Schmidt, "Optical atomic clocks", *Rev. Mod. Phys.*, vol. 87, pp. 637–701, 2 Jun. 2015. DOI: 10.1103/RevModPhys.87.637.
- [2] M. J. Thorpe, D. Balslev-Clausen, M. S. Kirchner, and J. Ye, "Cavity-enhanced optical frequency comb spectroscopy: Application to human breath analysis", *Opt. Express*, vol. 16, no. 4, pp. 2387–2397, Feb. 2008. DOI: 10.1364/OE.16.002387.

- [3] E. Obrzud, M. Rainer, A. Harutyunyan, *et al.*, "A microphotonic astrocomb", *Nature Photonics*, vol. 13, no. 1, pp. 31–35, Jan. 2019. DOI: 10.1038/s41566-018-0309-y.
- [4] A. Jørgensen, D. Kong, M. Henriksen, *et al.*, "Petabit-per-second data transmission using a chip-scale microcomb ring resonator source", English, *Nature Photonics*, vol. 16, pp. 798–802, 2022. DOI: 10.1038/s41566-022-01082-z.
- [5] A. S. Raja, S. Lange, M. Karpov, *et al.*, "Ultrafast optical circuit switching for data centers using integrated soliton microcombs", *Nature Communications*, vol. 12, no. 5867, 2021. DOI: 10.1038/s41467-021-25841-8.
- [6] L. Stern, J. R. Stone, S. Kang, *et al.*, "Direct kerr frequency comb atomic spectroscopy and stabilization", *Science Advances*, vol. 6, no. 9, eaax6230, 2020. DOI: 10.1126/sciadv.aax6230.
- [7] Y. Okawachi, K. Saha, J. S. Levy, Y. H. Wen, M. Lipson, and A. L. Gaeta, "Octave-spanning frequency comb generation in a silicon nitride chip", *Opt. Lett.*, vol. 36, no. 17, pp. 3398–3400, Sep. 2011. DOI: 10.1364/OL.36.003398.
- [8] E. Tagkoudi, D. Grassani, F. Yang, C. Herkommer, T. Kippenberg, and C.-S. Brès, "Parallel gas spectroscopy using mid-infrared supercontinuum from a single si3n4 waveguide", *Opt. Lett.*, vol. 45, no. 8, pp. 2195–2198, Apr. 2020. DOI: 10.1364/OL.390086. [Online]. Available: <https://opg.optica.org/ol/abstract.cfm?URI=ol-45-8-2195>.
- [9] C. Wang, T. Herr, P. Del'Haye, *et al.*, "Mid-infrared optical frequency combs at 2.5  $\mu\text{m}$  based on crystalline microresonators", English, *Nature Communications*, vol. 4, Jan. 2013, ISSN: 2041-1723. DOI: 10.1038/ncomms2335.
- [10] Z. Gong, X. Liu, Y. Xu, *et al.*, "Soliton microcomb generation at 2  $\mu\text{m}$  in z-cut lithium niobate microring resonators", *Opt. Lett.*, vol. 44, no. 12, pp. 3182–3185, Jun. 2019. DOI: 10.1364/OL.44.003182.
- [11] J. Li, H. Lee, K. Y. Yang, and K. J. Vahala, "Sideband spectroscopy and dispersion measurement in microcavities", *Opt. Express*, vol. 20, no. 24, pp. 26337–26344, Nov. 2012. DOI: 10.1364/OE.20.026337.
- [12] T. Herr, V. Brasch, J. D. Jost, *et al.*, "Temporal solitons in optical microresonators", *Nature Photonics*, vol. 8, no. 2, pp. 145–152, Feb. 2014. DOI: 10.1038/nphoton.2013.343.
- [13] Y. Zhao, L. Chen, C. Zhang, *et al.*, "Soliton burst and bi-directional switching in the platform with positive thermal-refractive coefficient using an auxiliary laser", *Laser & Photonics Reviews*, vol. 15, no. 11, p. 2100264, 2021. DOI: <https://doi.org/10.1002/lpor.202100264>.